Research Square

Preprints are preliminary reports that have not undergone peer review.
They should not be considered conclusive, used to inform clinical practice,
or referenced by the media as validated information.

Heat Transfer Enhancement in MHD Nanofluids Through Porous Cylindrical Annuli

R. Mahesha

mahesha41292@gmail.com

Atria Institute of Technology

N. Nalinakshi

Atria Institute of Technology

T. Sravan Kumar

Atria Institute of Technology

Research Article

Keywords: MHD, radiation effect, concentric cylinder, Forcheimer drag, Bruggemann model, heat sink.

Posted Date: August 5th, 2026

DOI: https://doi.org/10.21203/rs.3.rs-10448657/v1

License: This work is licensed under a Creative Commons Attribution 4.0 International License.
Read Full License

Additional Declarations: No competing interests reported.

Heat Transfer Enhancement in MHD Nanofluids Through Porous Cylindrical Annuli

R. Mahesha[1*, 2], N. Nalinakshi[1, 2], T. Sravan Kumar[1, 2]

[1]Department of Mathematics, Atria Institute of Technology, Bengaluru-560024, KA, India.
[1]Email: mahesha41292@gmail.com, ORCID ID:0009-0007-3982-2828
[2]Email: nalinigcm12@gmail.com ORCHID:0000-0001-8731-515X
[2]Visveswaraya Technological University, Belagavi – 560018, KA, India.
[2]Email: thavadasravankumar@gmail.com, ORCID ID: 0000-0002-4620-5103
*Corresponding author: *mahesha41292@gmail.com*

Abstract

This study investigates the MHD flow and heat transfer performance of ethylene glycol ($C_2H_6O_2$) – Silver (Ag) nanofluids between two concentric cylinders, by incorporating the effects of thermal radiation, internal heat sink, viscous dissipation, and porous media. A comparative analysis is performed using the Maxwell-Garnett and Patel models to evaluate nanofluid thermal conductivity enhancements. The interplay of external magnetic fields and nanoparticle dispersion introduces complex thermal-fluid dynamics, influencing energy transport significantly. A set of highly nonlinear ordinary differential equations governing the momentum and energy balance is derived and solved using the BVP4C numerical method in MATLAB. The study analyses the influence of key dimensionless parameters such as Hartmann number, radiation parameter, Eckert number, and nanoparticle volume fraction on flow velocity and temperature profiles. Results show that the Bruggemann model predicts higher heat transfer rates compared to the Maxwell - Garnett model, especially at elevated nanoparticle concentrations. The presence of MHD and radiation effects enhances thermal boundary layer development, offering better control of heat transfer. This comparative investigation offers critical insights for optimizing thermal systems in nuclear cooling, biomedical applications, and energy-efficient industrial processes, providing a foundation for the design of advanced thermal management technologies in cylindrical geometries under MHD influences.

Key words: MHD, radiation effect, concentric cylinder, Forcheimer drag, Bruggemann model, heat sink.

1. Introduction

Heat transfer refers to the process of transferring thermal energy, by converting it into mechanical energy, to enhance efficiency of various thermal systems. Improving heat transfer efficiency remains a critical challenge in industrial and engineering applications. One promising approach to address this challenge involves the use of nanofluids, which have shown

significant potential in both heating and cooling processes due to their superior thermal properties. Nanofluids are suspensions of nanoparticles in base fluids it exhibits enhanced thermal conductivity, improved viscosity behaviour, and better stability, making them ideal for high-performance heat transfer applications. The pioneering work by Choi and Eastman [1] first introduced the concepts of nanofluids and highlighted their role in enhancing heat transfer performance. Mixed convection, which involves the combined effects of natural and forced convection, was systematically investigated by Ali et al. [2], the flow behaviour of vertical surface in a saturated porous medium. Sunder et al. [3], explored natural convection over a vertically heated plate under the influence of an external magnetic field, analysing its effects on both heat and mass transfer. Mahros & Aly [4], examined numerical simulations on MHD flows in the influence of nanofluids.

Comparative analysis of numerical and analytical studies has been conducted in the influence of MHD free convection of heat and mass transfer process. Roopa et al. [5] examined numerical analysis of free convection MHD flow over a moving vertical flat plate. Nayak et al. [6] analyzed the effects of MHD, thermal radiation, and heat generation/absorption on heat and mass transfer in free convection over a stretching sheet. As a result, provide that boundary layer thickness increases with increment in fluid viscosity, in controlling thermal and momentum boundary layers. MHD flow over a cylindrical geometry were carried out by finite element method [7, 8], it shows that magnetic field oppose the fluid motion, thereby reducing the flow rate. These studies also considered the effects of different nanoparticles, contributing to a better understanding of nanofluid behaviors under magnetic field. Saranya and Al-Mdallal [9] investigated unsteady, non-Newtonian MHD flow with in a contracting cylindrical channel, as a result shows that the presence of MHD enhances the fluid flow rate and that CoFe2O4 nanofluids significantly improve heat transfer performance. The influence of non-linear electrified jets in the electrospinning process was modeled using a bead-spring approach by Hasan [10]. The simulation indicated that the elongation of the jet reduces the length of stable jet formation, a crucial factor in nanofiber production. Umavathi et al. [11] examined the combined effects of thermal radiation and MHD on Casson nanofluid flow over a stretching surface near a convective stagnation point. Using numerical method results shows that Sherwood number is significantly influenced by Brownian motion, emphasizing the important of nanoparticle dynamics in convective mass transfer.

Magnetohydrodynamics (MHD), involving the motion of electrically conducting fluids under the influence of a magnetic field, has been extensively explored in the context of nanofluids. In a complementary study, Saranya et al. [12] performed a numerical analysis on

unsteady hybrid nanofluid flow with ferroparticles in the cylindrical geometry, employing the numerical techniques while accounting for viscous and ohmic dissipation effects their findings indicate a reduction in both the heat transfer rate and skin friction coefficient with increasing Eckert number. Umavathi & Shamshuddin [13] investigated a comprehensive analysis to solve nonlinear vibration equations foe single-walled carbon nanotubes, it shows that vibrational frequency increases with amplitude. Alhefthi et al. [14] analyzed the motion of nanoscale droplets in incompressible Newtonian fluids, showing that droplet sphericity plays a crucial role in modulating velocity and acceleration. Mahesha et al. [15] examined natural convection of Cu-water nanofluids confined between two parallel plates, concluding that the thermal boundary layer thickness decreases with increasing nanoparticle volume fraction, it enhancing convective efficiency.

Analysis of oscillatory behavior of a rigid rod on a circular surface is examined by Rajeev et al. [16], it shows the results that oscillation amplitudes diminish with increasing time, it reaches peak velocity at t = 600s. Sankari et al. [17] investigated a theoretical study on the dynamic response of single walled cardon nanotubes, employing a Pasternak – type foundation model. The result shows that higher nonlocal parameters significantly enhance the velocity distribution along the nanotube structure. Temperature dependent heat transfer in both solid and porous convective fins, by varying thermal conductivity and internal heat generation are solved by semi analytical method [18, 19], and demonstrated the superior thermal efficiency and accuracy. Khan et al. [20] analyzed analytical exp-function method to solve nonlinear wave equations such as the Sine-Gordon and Ostrovsky equations, successfully validating the methods through contour plots of the resulting velocity fields. Gosty et al. [21] studied nanofluid flow within two concentric cylinders governed by considering MHD and thermal radiation effects. The result shows that Eckert number and Reynolds number positively influence temperature profiles. Mixed convective flow over a nonlinear stretching surface embedded with gyrotactic microorganisms in heat and mass transfer with Brownian motion and thermophoresis effects. The results illustrate that magnetic parameters significantly retard the flow rate is analyzed by Kumar [22]. In a related study, Naz and Sohail [23] examined MHD flow and heat transfer over a stretching cylinder using analytical and numerical techniques, revealing that increment in magnetic parameter led to a noticeable decline in velocity profile.

A numerical investigation on MHD flow of nanofluids influenced by thermal radiation over a stretching surface is examined by Ghasemi and Hatami [24]. The analysis revealed that high-accuracy solutions, with thermal boundary layer thickness increases by increment in Biot

number. Gouran et al. [25] analyzed MHD flow and thermal radiation effects over two concentric cylinders, as a result shows that Nusselt number and thermal performance are increased by increment in Hartmann number. Peng et al. [26] studied heat transfer in a rotating horizontal annulus under the influence of MHD and thermal radiation using Koo-Kleinstreuer-Li model. Sravan Kumar et al. [27] examined the velocity profile increases significantly when the magnetic field is oriented perpendicular to the fluid motion, in a frame of reference fixed relative to the plate. Babu et al. [28] analysed mixed convection MHD flows over a vertically heated plate embedded in a porous matrix with variable fluid properties. Mahesha et al. [29] investigated MHD, internal heat generation/absorption over a two concentric annulus are considered. As a result, shows that enhanced heat transfer was observed.

Based on the above literature survey research has been devoted to heat transfer in concentric cylindrical annulus with MHD, thermal radiation, internal heat generation or absorption, Forchheimer Drag, and ethylene glycol – Ag nanofluids. The influence of various nanoparticles on enhancing effective thermal conductivity, modulating fluid flow behaviour, and maximizing heat transfer performance impact of MHD forces and radiative heat flux. The practical implementation of advanced nanofluid-porous medium in hyperthermia cancer therapy, nuclear reactor thermal regulation to MHD power systems, biomedical heat management. The current numerical framework encapsulating these multifaceted interactions highlights a critical gap in the literature. The development of predictive, coupled Multiphysics models is imperative for advancing the understanding and technological deployment of nanofluid-based heat transfer systems in complex engineering and biomedical environments.

2. Mathematical Formulation

Consider a steady, laminar flow of an incompressible ethylene glycol – Silver based nanofluids confined between two concentric annuli. The fluid flow is directed along the axial Z - axis, in the radial coordinate acts upwards. By assuming induced magnetic field is ignored and Lorentz force is applied perpendicular to the fluid flow direction. Impact of internal heat generation, thermal radiation, and Forcheimer drag over two concentric cylinders containing nano with porous medium. The inner and outer cylinder are maintained at constant temperatures, T_1 is temperature for r_1, T_2 is temperature for r_2 between two cylinders containing porous nanofluids. In this current problem, the governing equations of Ag - $C_2H_6O_2$ nanofluids and heat transfer in cylindrical coordinate system with boundary conditions [21, 26] are given by

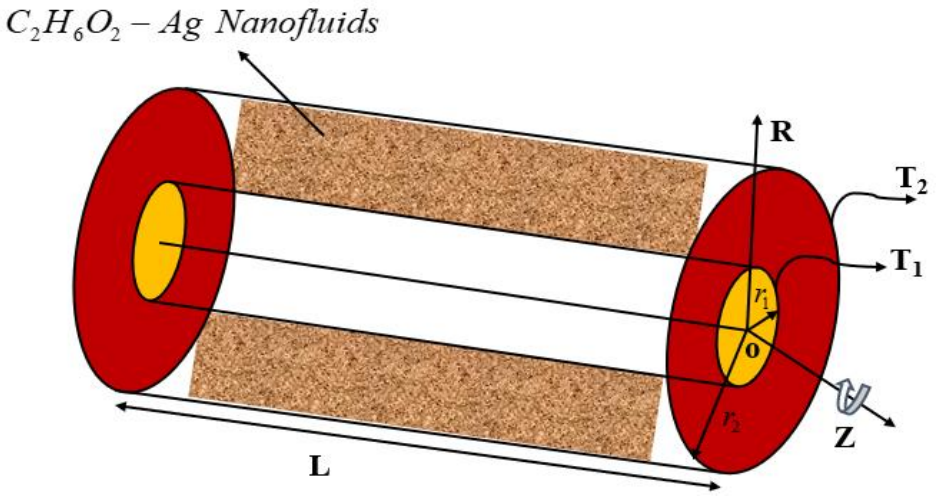


Fig 1. Physical configuration flow problem.

Conservation of mass

$$\frac{1}{R}\left(\frac{\partial}{\partial R}(RU)\right)=0 \tag{1}$$

Conservation of momentum

$$\upsilon_{nf}\left(\frac{\partial^2 U}{\partial R^2}+\frac{1}{R}\frac{\partial U}{\partial R}-\frac{U}{R^2}\right)-\frac{\sigma_{nf}UB_0^2}{\rho_{nf}}-\frac{U\mu_{nf}}{k\rho_{nf}}-\frac{\phi C_b}{\sqrt{k}}U^2=U\frac{\partial U}{\partial R} \tag{2}$$

Conservation of energy

$$\frac{\kappa_{nf}}{R}\frac{\partial}{\partial R}\left(R\frac{\partial T}{\partial R}\right)+\mu_{nf}\left(\frac{\partial U}{\partial R}-\frac{U}{R}\right)^2-\frac{\partial q_r}{\partial R}-Q_0\left(T-T_2\right)+\frac{\phi C_b}{\sqrt{k}}U^3=\left(\rho C_p\right)_{nf}U\frac{\partial T}{\partial R} \tag{3}$$

Subjected to the boundary conditions is imparted

$$R=r_1 : U\left(R\right)=\omega r_1,\ T=T_1$$

$$R=r_2 : U\left(R\right)=0,\ T=T_2 \tag{4}$$

Using the Taylors series expansion and Rosseland approximation heat flux rate of radiation is given by

$$T^4 \cong 4T_2^3T-3T_2^4,\ q_r=-\frac{4\sigma_e}{3\beta_R}\frac{\partial T^4}{\partial R},\ \frac{\partial q_r}{\partial R}=-\frac{4\sigma_e 4T_2^3}{3\beta_R}\frac{\partial^2 T}{\partial R^2} \tag{5}$$

Substituting equation (5) in equation (3), the modified energy equation becomes

$$\frac{\kappa_{nf}}{R}\frac{\partial}{\partial R}\left(R\frac{\partial T}{\partial R}\right)+\mu_{nf}\left(\frac{\partial U}{\partial R}-\frac{U}{R}\right)^2+\frac{4\sigma_e 4T_2^3}{3\beta_R}\frac{\partial^2 T}{\partial R^2}-Q_0\left(T-T_2\right)+\frac{\phi C_b}{\sqrt{k}}U^3=\left(\rho C_p\right)_{nf}U\frac{\partial T}{\partial R} \tag{6}$$

The non-dimensional transformation of above governing equations [21, 26] are

$$r=\frac{R}{r_2},\ u=\frac{U}{\omega r_1},\ \eta=\frac{r_1}{r_2},\ \theta=\frac{T-T_2}{T_1-T_2} \tag{7}$$

The non-dimensional parameters are

$$\mathrm{Re}=\frac{\rho_f \omega r_1 r_2}{\mu_f},\ \mathrm{Pr}=\frac{\mu_f\left(\rho C_p\right)_f}{\rho_f \kappa_f},\ Ec=\frac{\rho_f\left(\omega r_1\right)^2}{\left(\rho C_p\right)_f \Delta T},\ R=\frac{4\sigma_e T_c^3}{\beta_R \kappa_f},\ Ha=B_0 d\sqrt{\frac{\sigma_f}{\mu_f}},\ Da=\frac{k}{r_2^2}$$

$$Q=\frac{Q_0 r_2^2}{\kappa_f},\ S_1=\frac{\rho_{nf}}{\rho_f},\ S_2=\frac{\mu_{nf}}{\mu_f},\ S_3=\frac{\left(\rho C_p\right)_{nf}}{\left(\rho C_p\right)_f},\ S_4=\frac{\kappa_{nf}}{\kappa_f},\ S_5=\frac{\sigma_{nf}}{\sigma_f},\ \eta=\frac{r_1}{r_2},\ Fr=\frac{C_b}{\sqrt{k}} \tag{8}$$

After the non - dimensional analysis dimensionless equations are given by

$$\frac{\partial^2 u}{\partial r^2}+\frac{1}{r}\frac{\partial u}{\partial r}-\left\{\frac{Ha^2}{\left(1-\eta^2\right)}\frac{S_5}{S_2}+\frac{1}{r^2}\right\}u-\frac{u}{Da}-\frac{S_1}{S_2}Fr\,u^2-\mathrm{Re}\frac{S_1}{S_2}u\frac{\partial u}{\partial r}=0 \tag{9}$$

$$\frac{\partial^2 \theta}{\partial r^2}+\frac{1}{r}\frac{\partial \theta}{\partial r}+Ec\,\mathrm{Pr}\frac{S_2}{S_4}\left\{\frac{\partial u}{\partial r}-\frac{u}{r}\right\}^2+\frac{4}{3}\frac{R}{S_4}\frac{\partial^2 \theta}{\partial r^2}-\frac{Q}{S_4}\theta+\frac{Ec\,Fr}{S_4}u^3-\mathrm{Pr}\,\mathrm{Re}\frac{S_3}{S_4}u\frac{\partial \theta}{\partial r}=0 \tag{10}$$

Dimensionless boundary conditions are imparted

$$r=\eta: u=1,\ \theta=1$$

$$r=1: u=0,\ \theta=0 \tag{11}$$

Non-dimensional Skin friction and Nusselt number is given by

$$C_f=-S_2\left.\frac{\partial u}{\partial r}\right|_{r=\eta} \quad Nu=-S_4\left(1+\frac{4N}{3S_4}\right)\left.\frac{\partial \theta}{\partial r}\right|_{r=\eta} \tag{12}$$

Table 1: Thermophysical properties of spherical-shaped nanofluids [27].

Properties	**Formulas**
Heat capacitance	$\left(\rho C_p\right)_{nf}=\left(1-\phi\right)\left(\rho C_p\right)_f+\phi\left(\rho C_p\right)_s$
Thermal expansion coefficients	$\left(\rho\beta\right)_{nf}=\left(1-\phi\right)\left(\rho\beta\right)_f+\phi\left(\rho\beta\right)_s$
Thermal diffusivity	$\alpha_{nf}=\frac{\kappa_{nf}}{\left(\rho C_p\right)_{nf}}$
Density variation	$\rho_{nf}=\left(1-\phi\right)\rho_f+\phi\rho_s$
Dynamic viscosity	$\mu_{nf}=\frac{\mu_f}{\left(1-\phi\right)^{2.5}}$
Thermal conductivity (Maxwell-Garnett Model)	$\kappa_{nf}=\kappa_f\left(\frac{2\kappa_f-2\phi\left(\kappa_f-\kappa_s\right)+\kappa_s}{2\kappa_f+\phi\left(\kappa_f-\kappa_s\right)+\kappa_s}\right)$
Electrical conductivity	$\sigma_{nf}=\sigma_f\left(1+\frac{3\left(\sigma-1\right)\phi}{\left(\sigma+2\right)-\left(\sigma-1\right)\phi}\right)$

Bruggeman model [30] for spherical shaped nanoparticles of thermal conductivity is given by

$$\frac{\kappa_{nf}}{\kappa_f}=\frac{(3\phi-1)\frac{\kappa_s}{\kappa_f}+\{3(1-\phi)-1\}+\sqrt{\Delta}}{4} \text{ where } \Delta=\left[(3\phi-1)\frac{\kappa_s}{\kappa_f}+\{3(1-\phi)-1\}\right]^2+8\frac{\kappa_s}{\kappa_f} \quad (13)$$

3. Numerical Solution

The non-dimensional, non-linear and coupled boundary value problem represented by equations (9 - 11), governing the flow and thermal fields of Ag - $C_2H_6O_2$ nanofluid between two concentric cylinders, is solved numerically using the BVP4C solver in MATLAB software. This solver is suitable for to solve complex system of boundary value problems involving porous media, thermal radiation, MHD, internal heat sink effects. To facilitate the application of the BVP4C algorithm, the governing second-order differential equations are transformed into an equivalent system of first-order ordinary differential equations. This method, form the set of 1st order ODE's $y_1=r,\ y_2=u,\ y_3=u',\ y_4=\theta,\ y_5=\theta'$. With the algorithm and corresponding BCs is

$$\begin{pmatrix} y_1' \\ y_2' \\ y_3' \\ y_4' \\ y_5' \end{pmatrix}=\begin{pmatrix} 1 \\ y_3 \\ \frac{-y_3}{y_1}+\frac{y_2}{y_1}+\frac{Ha^2}{\left(1-\eta^2\right)}\frac{S_5}{S_2}y_2+\frac{y_2}{Da}+\frac{\mathrm{Re}\,S_1}{S_2}y_2y_3+\frac{S_1}{S_2}F\,y_2^2 \\ y_4 \\ \frac{1}{\left(1+\frac{4}{3}\frac{N}{S_4}\right)}\left(\frac{-y_5}{y_1}-\frac{Ec\,\mathrm{Pr}\,S_2}{S_4}\left(y_3-\frac{y_2}{y_1}\right)^2+\frac{Q\,y_4}{S_4}+\frac{\mathrm{Pr}\,\mathrm{Re}\,S_3y_2y_5}{S_4}-\frac{Ec\,Fr}{S_2}y_2^3\right) \end{pmatrix} \quad (14)$$

and related boundary conditions is $\begin{pmatrix} y_1 \\ y_2 \\ y_3 \\ y_4 \\ y_5 \end{pmatrix}=\begin{pmatrix} \eta \\ 1 \\ u_1 \\ 1 \\ \theta_1 \end{pmatrix}$.

To obtain a convergent solution, initial estimates for unknown parameters such as $y_1=r,\ y_2=u,\ y_3=u',\ y_4=\theta,\ y_5=\theta'$ are arbitrary chosen. These estimates are refined iteratively using the BVP4C method, which provides numerical approximations with high accuracy. The iterative procedure also involves determining an appropriate maximum value of η, ensuring that the asymptotic conditions $R=r_1: U(R)=\omega r_1,\ T=T_1$ and $R=r_2: U(R)=0,\ T=T_2$ are satisfied. A trial-and-error approach is used to refine the guesses

for unknowns, followed by an iterative correction process to meet the convergence criteria. The error tolerance is set to 10^{-6} to ensure the numerical stability and accuracy. For all computations, a step size of $\Delta\eta = 0.01$ is used balancing computational efficiency with solution accuracy.

Table 2: Numerical values of physical properties of ethylene glycol and different nanoparticles [27].

Property	**Ethylene Glycol** $C_2H_6O_2$	**Water** H_2O	**Ag**	**Cu**	**CuO**
$\rho\left(kgm^{-3}\right)$	1052.1	997.1	10500	8933	6320
$\mu\left(Pa\,s\right)$	0.0031871	0.00089	-	-	-
$\kappa\left(W\,m^{-1}K^{-1}\right)$	0.432	0.613	429	401	76.5
$\beta\times10^{-5}\left(K^{-1}\right)$	57	21	1.89	1.67	1.80
$C_p\left(J\,kg^{-1}\,K^{-1}\right)$	3301.7	4179	235	305	531.8
$\sigma\left(\omega m\right)^{-1}$	1.24×10^{-6}	5.5×10^{-6}	63×10^{-6}	58×10^{-6}	0.1×10^{-6}

4. Graphical Results and Discussion

The non-dimensional equations of (9 - 11), representing the flow and thermal behavior of nanofluids between two concentric cylinders, are numerically solved using the BVP4C technique in MATLAB. These equations are non-linear and coupled in nature, using Table 2, Ag - $C_2H_6O_2$ dimensionless BCs. The solutions are plotted velocity and temperature profiles Figs. (2 – 19) keeping parameters constants such as $Da = 1,\ Q = 1, Ha = 1,\ F = 0.5\ Ec = 0.01,$ $R = 0.1,\ \phi = 0.01, \Pr = 6.8,\ \eta = 0.5,\ \mathrm{Re} = 1$.

4.1. Effect of volume fraction (ϕ)

From figures (2 & 3) provide the analysis of concentration of nanoparticles in velocity and temperature profiles. We observed that an increment in volume fraction velocity increases in Fig. 2 due to increased viscosity leads to overall density becomes higher due to the presence of heavier Ag nanoparticles. In buoyancy-driven flows, these changes can intensify thermal gradients and enhance mixed convection. The stronger thermal gradient leads to more vigorous buoyancy force, which contributes to increasing the fluid velocity. In Fig. 3 an increment in volume fraction temperature decreases because silver has an extremely high thermal conductivity with base fluid ($C_2H_6O_2$) as a result in enhanced thermal conductivity allows the fluid to conduct and dissipate heat transfer, it leads to reduction in the bulk fluid temperature

during heat transfer processes. These effects beneficial in thermal management system, microchannel heat exchangers, and electronic cooling.

4.2. Effect of Forchheimer Drag (Fr).

In the analysis of Forchheimer drag force with momentum and energy equations of Ag - $C_2H_6O_2$ in figures 4 & 5. An increase in the Forchheimer drag force leads to greater inertial resistance in the porous medium. These causes decrease in nanofluid velocity, especially in dense and viscous fluids. As convective transport is weakened, the temperature distribution also drops due to less effective heat transfer. The dual reduction in velocity and temperature is a direct result of enhanced porous medium resistance and inhibited flow dynamics. This effects applicable in the cooling, thermal insulation, catalytic reactors and chemical filters.

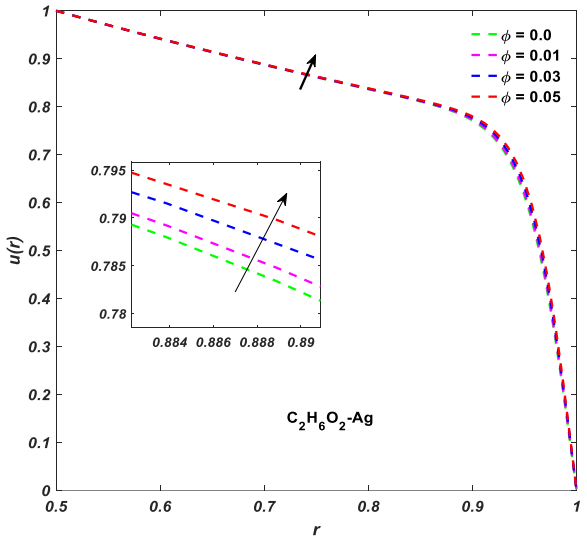


Fig. 2: Variation of ϕ on velocity.

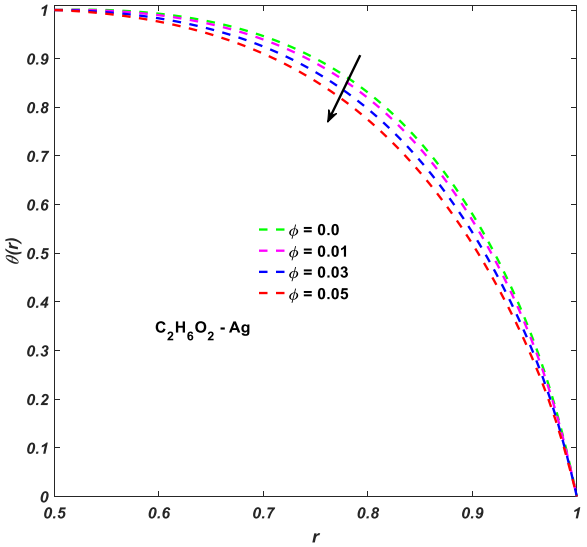


Fig. 3: Variation of ϕ on temperature.

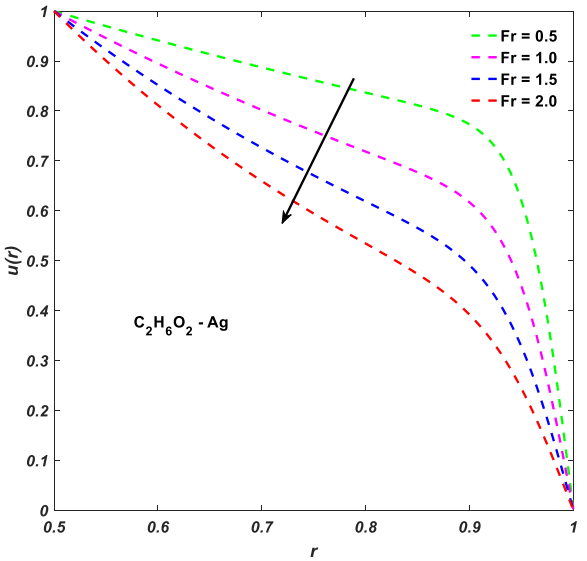


Fig. 4: Variation of Fr on velocity.

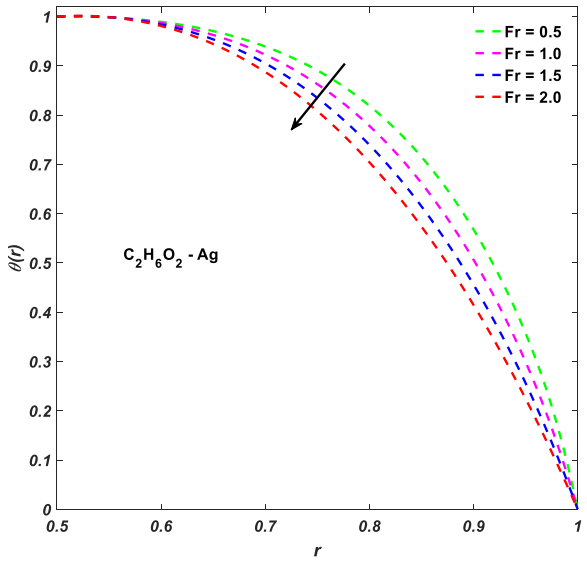


Fig. 5: Variation of Fr on temperature.

4.3. Effect of Hartmann number or MHD (Ha).

In an Ag - $C_2H_6O_2$ nanofluid, increment in Hartmann number (Ha) leads to decrease in velocity and temperature figures 6 & 7. This is due to the Lorentz force generated by the magnetic field, which opposes fluid motion and suppresses convective heat transfer. Since silver has high electrical conductivity, the fluid becomes more resistive to magnetic effects, enhancing the damping. As a result, flow slow down and heat transport is reduced, causing overall velocity and temperature drop. It is useful in the field of high heat conductivity, precise magnetic control, and stable thermal regulation, and medical systems.

4.4. Effect of Darcy parameter (Da).

From figures 8 & 9 shows that variation of Darcy number with velocity and temperature profiles. In porous media, Darcy number signifies the relative permeability of the medium. Darcy number increases, it means the medium becomes more porous, offering less resistance to the flow. In Ag - $C_2H_6O_2$ nanofluid, which combines high thermal conductivity of silver nanoparticles and low viscosity of ethylene glycol, the fluid can move freely through the medium as the resistance drops. This results in a noticeable increase in velocity due to enhanced momentum transfer in Fig. 8. As the velocity of nanofluid increases, convective heat transfer is intensified in Ag nanoparticles and rapid distribution of thermal energy. Thermal boundary layer becomes thinner, which allows better heat absorption from heated surfaces. This leads to an overall increase in temperature from Fig. 9. These findings are applicable in energy storage systems, medical therapies.

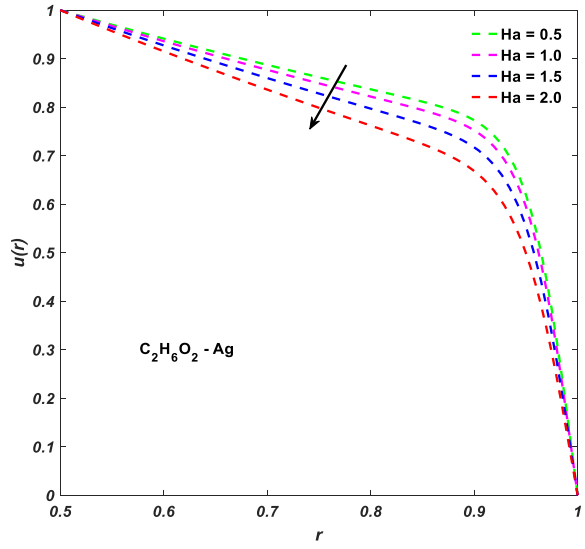


Fig. 6: Variation of *Ha* on velocity.

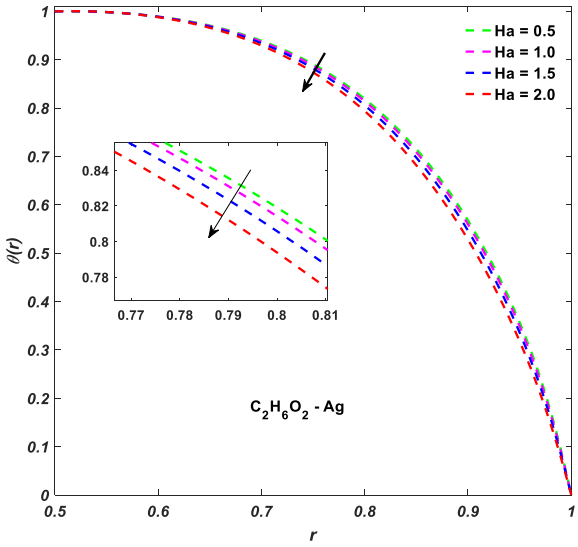


Fig. 7: Variation of *Ha* on temperature.

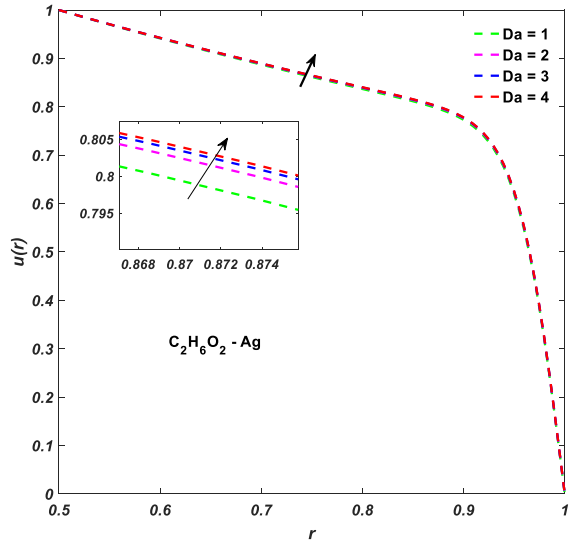


Fig. 8: Variation of *Da* on velocity.

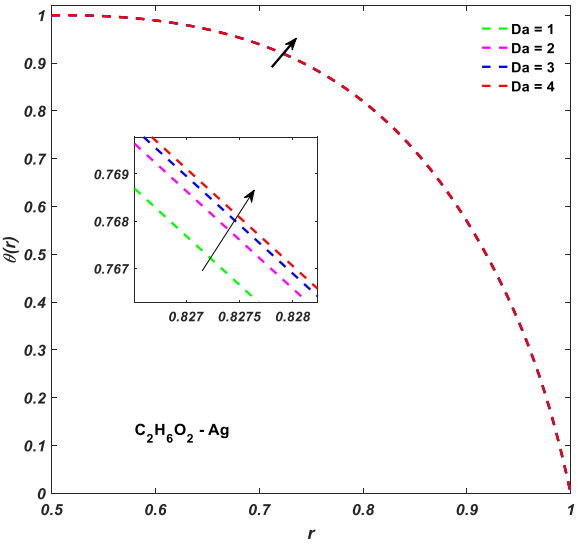


Fig. 9: Variation of *Da* on temperature.

4.5. Effect of Reynolds number (Re).

The behavior of Reynolds number (*Re*) in fluid flow analysis of momentum and energy is observed in figures 10 & 11. Reynolds number increases in an Ag - $C_2H_6O_2$ nanofluid, both the velocity and temperature profiles tend to increase. This is due to the dominance of inertial forces over viscous forces. As the Reynolds number is directly proportional to flow velocity, an increase in Re gives a faster – moving fluid, which leads to less resistance due to reduced viscous effects. Temperature also increases with higher Reynolds number in Ag - $C_2H_6O_2$ nanofluid flows due to improved convective heat transfer. The rate at which heat is transported form heated surfaces into the fluid, thinning thermal boundary layer and raising local temperature gradients. To improve overall thermal efficiency by boosting both flow rate and heat transfer performance in microchannel based cooling systems.

4.6. Effect of aspect ratio parameter (η).

The aspect ratio η plays a significant role in determining velocity and temperature distributions from figures 12 & 13. As η increases, it indicates that the space between concentric boundaries becomes narrower, thereby restricting the flow channel. A higher aspect ratio causes an increase in viscous resistance within the narrowed flow domain. This elevated resistance slows down the fluid motion due to increased wall shear stresses, leading to a noticeable reduction in velocity graph Fig. 12. As a result, less thermal energy is transported by the nanofluid along the flow direction, silver nanoparticles possess high thermal conductivity which enhances heat transfer capacity of the base fluid. Dominant conduction in narrow channels and reduced velocity suppresses leads to thermal boundary layer development and minimizes convective enhancement. It is used in microchannel heat sinks, cryogenic tank insulation, and thermal management in electronic devices.

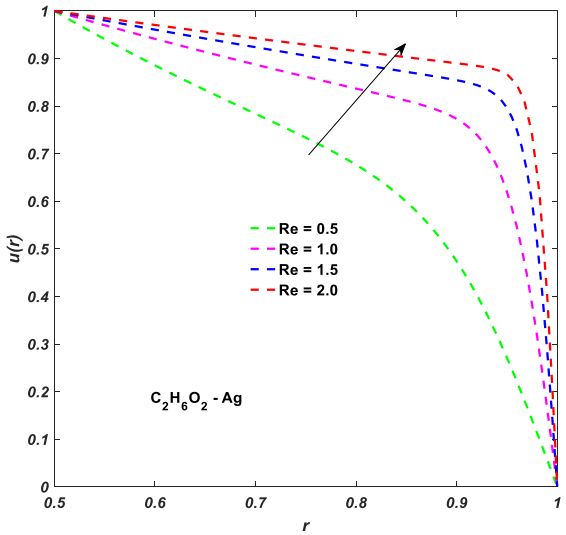


Fig. 10: Variation of Re on velocity.

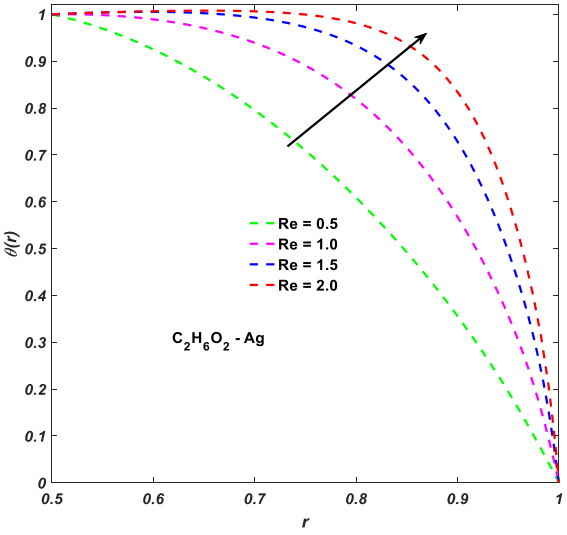


Fig. 11: Variation of Re on temperature.

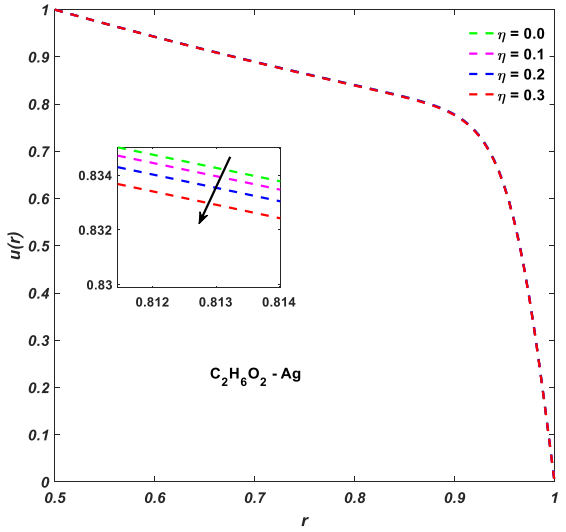


Fig. 12: Variation of η on velocity.

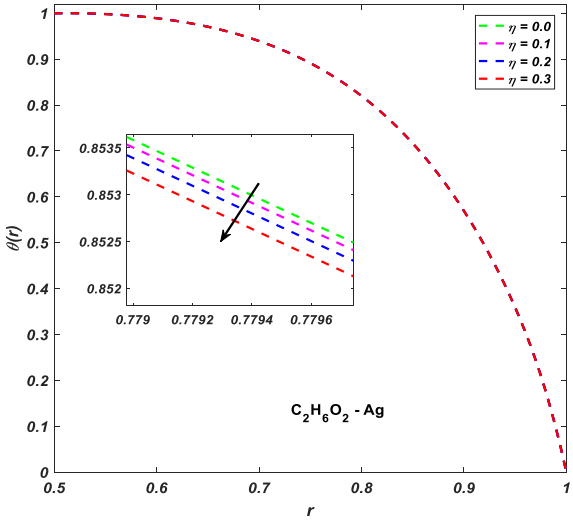


Fig. 13: Variation of η on temperature.

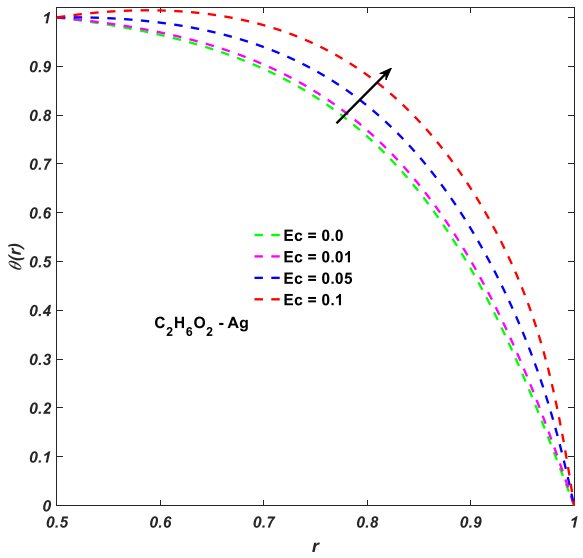


Fig. 14: Variation of Ec on temperature.

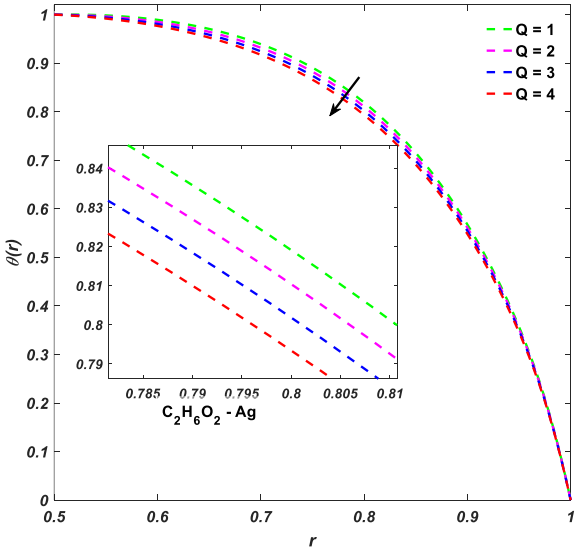


Fig. 15: Variation of Q on temperature.

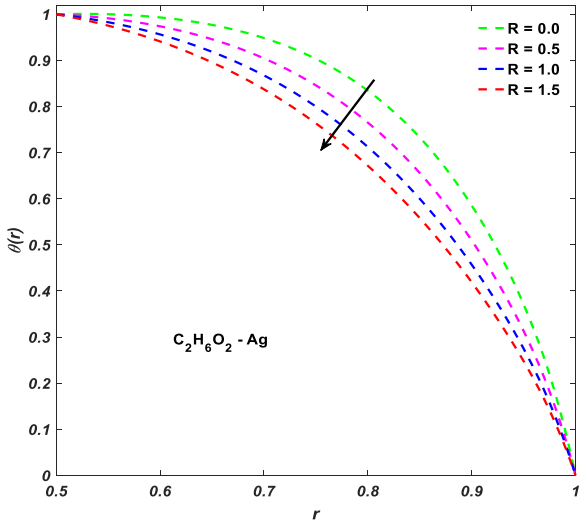


Fig. 16: Variation of R on temperature.

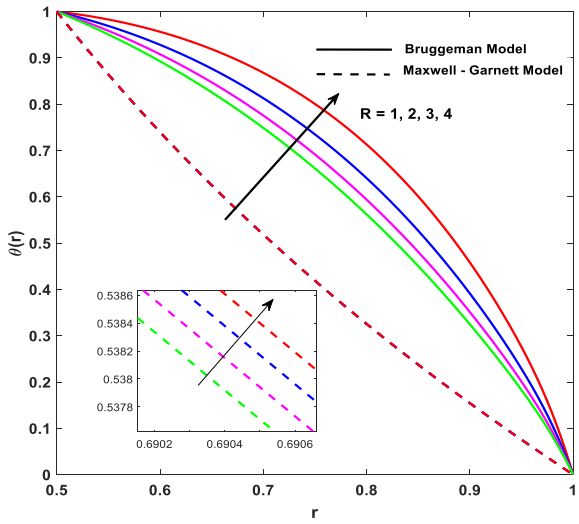


Fig. 17: Comparison of thermal conductivity model on temperature.

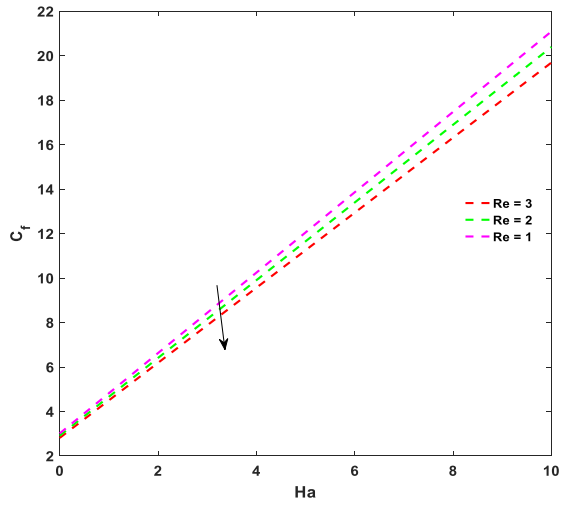


Fig. 18: Effect of Skin friction and Hartmann number on Reynolds number.

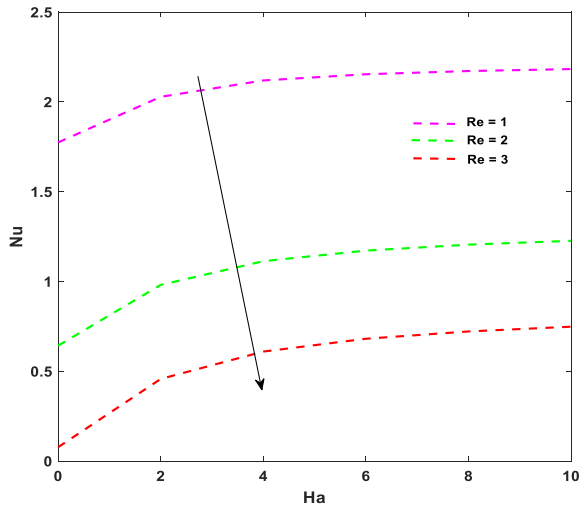


Fig. 19: Effect of Nusselt number and Hartmann number on Reynolds number.

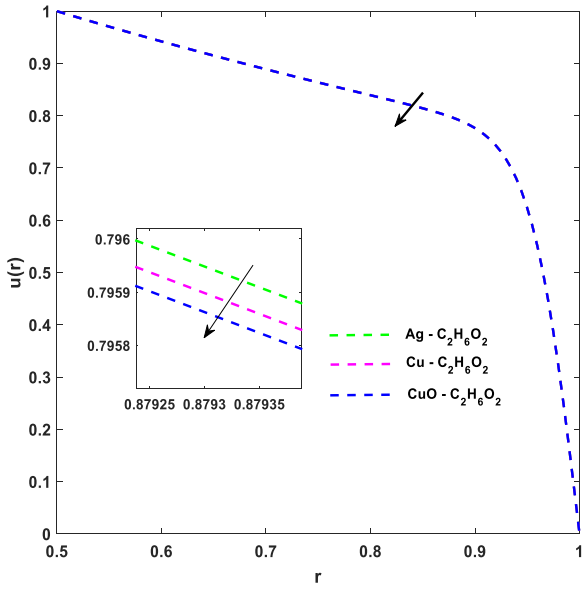


Fig. 20: Effect of different nanoparticles on velocity.

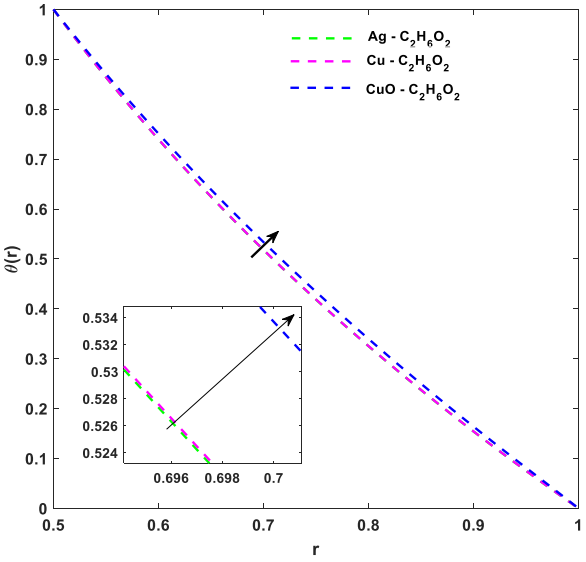


Fig. 21: Effect of different nanoparticles on temperature.

4.7. Effect of Eckert number (Ec)*, heat sink* (Q)*, thermal radiation* (R).

In Fig. 14. We observed that Ec increases temperature increases, due to internal friction during the fluid flow arises by viscous dissipation. This friction converts kinetic energy into thermal energy, in high viscosity fluids. Silver nanoparticles enhance heat absorption and thermal conductivity, amplifying temperature increment. From Fig. 15 analyzed the heat absorption parameter, as Q increases temperature profile decreases due to absorption of internal energy of the fluid it leads to lowering its temperature. In thermal radiation facilitates energy loss in the form of electromagnetic waves. Silver is one of the best thermal conductors, faster heat dissipation from hotter to cooler regions is observed in Fig. 16 and its applications are in biomedical devices, solar thermal systems.

4.8. Comparison of thermal conductivity models.

From the Fig. 17 we analyzed Bruggemann model gives better thermal performance compared to Maxwell – Garnett model by varying radiation parameter. As R increases, the temperature decreases across the domain, it shows stronger radiative heat loss leads thermal radiation cools the system more effectively. Bruggeman model predict higher temperature than Maxwell – Garnett model, as a result greater effective thermal conductivity, allowing smoother heat distribution.

4.9. Effect of Skin friction and Nusselt number.

In the Figure 18 & 19, analyzed effect of skin friction and Nusselt number by varying Reynolds number with Harman number. As Reynolds number increases with Hartman number skin friction coefficient decreases because inertial forces dominate, reducing wall shear stress in Fig. 18. In contrast, Nusselt number indicates heat transfer coefficient in Fig. 19 observed that magnetic field enhances wall shear for higher Reynolds numbers suppress heat transfer rate and it is applicable in MHD cooling systems and heat exchangers.

4.10. Effect of different nanoparticles.

Analysis of different nanoparticles such as Silver (Ag), Copper (Cu), and Copper Oxide (CuO), on velocity and temperature profile in Fig. 20 & 21. In Fig. 20 observed that Ag - $C_2H_6O_2$ is high velocity than Cu - $C_2H_6O_2$ and CuO - $C_2H_6O_2$ due to high density and thermal conductivity of Ag comparatively Cu and CuO. In contrast, CuO nanofluids are more viscous and less conductive, which reduces the fluid flow. From Fig. 21 shows that Ag - $C_2H_6O_2$ is less temperature than Cu - $C_2H_6O_2$ and CuO - $C_2H_6O_2$ because of silver has superior thermal conductivity, which promotes efficient heat dissipation and cooling. On the other hand, CuO nanofluid retains more heat, resulting in a higher temperature distribution. The importance of nanoparticle in thermal management systems such as cooling jackets, microchannel heat exchangers, and nanofluid based energy devices.

In Table 3 shows that comparative study of existing work in the absence of Darcy number, heat sink parameter, and Forchheimer drag force results shows that are in good agreement.

Table 3: Comparison of the work for velocity and temperature Re=1, Ha=1, Ec=0.1, R=0.2, Da=0, Q=0, Fr=0.

r	Velocity			Temperature		
	Ghasemi & Hatami [24]	Peng et al. [26]	Present study	Ghasemi & Hatami [24]	Peng et al. [26]	Present study
0.5000	1.0000	1.0000	1.0000	1.0000	1.0000	1.0000
0.5072	0.9772	0.9772	0.9773	1.0001	1.0001	1.0001
0.5286	0.9128	0.9128	0.9129	0.9962	0.9962	0.9963
0.5628	0.8167	0.8167	0.8168	0.9781	0.9781	0.9782
0.6079	0.7010	0.7010	0.7011	0.9342	0.9342	0.9343
0.6613	0.5776	0.5776	0.5777	0.8562	0.8563	0.8564
0.7198	0.4558	0.4558	0.4559	0.7438	0.7439	0.7440
0.7801	0.3423	0.3423	0.3424	0.6049	0.6048	0.6050
0.8386	0.2415	0.2415	0.2416	0.4535	0.4535	0.4536
0.8920	0.1564	0.1564	0.1565	0.3063	0.3063	0.3064

0.9371	0.0887	0.0887	0.0888	0.1784	0.1784	0.1785
0.9713	0.0396	0.0396	0.0397	0.0809	0.0809	0.0810
0.9927	0.0097	0.0097	0.0098	0.0203	0.0203	0.0204
1.0000	0.0000	0.0000	0.0000	0.0000	0.0000	0.0000

5. Final Remarks

This study presents a comprehensive numerical investigation of thermal and flow behavior of Ag - $C_2H_6O_2$ nanofluid between two concentric cylinders using non-linear, coupled equations solved through BVP4C technique in MATLAB. The influencing parameters are Forchheimer drag force, Hartman number, Darcy number, Reynolds number, Eckert number, heat sink parameter, thermal radiation aspect ratio, skin friction and Nusselt number are systematically analyzed on velocity and temperature profiles.

- An improved thermal conduction is observed in nanofluids using nanoparticle volume fraction leads to a rise in fluid velocity.
- Magnetic field and Forchheimer drag shows a reduction in both velocity and temperature impose additional resistance and dampen convective motion.
- Enhanced heat transfer is observed in silver nanoparticles, due to their exceptionally high thermal conductivity and density to improve heat dissipation.
- Effect of Darcy number and Reynolds number significantly increase flow behavior and heat transfer rate.
- The improved heat transfer to influence internal energy distribution by Eckert number and thermal radiation effects, are highly suitable in microchannel heat sinks, electronic component cooling. And thermal energy storage systems.

Author Contributions: Mahesha R: Conceptualization(equal); Data curation (equal); Formal analysis (equal); Investigation (equal); Methodology (equal); Project administration (equal); Supervision (equal); Validation (equal); Visualization (equal); Writing–original draft (equal); Writing review & editing (equal). Nalinakshi N: Conceptualization (equal); Data curation (equal); Formal analysis (equal); Investigation (equal); Methodology (equal); Project administration (equal); Supervision (equal); Validation (equal); Visualization (equal); Writing–original draft (equal); Writing–review & editing(equal). Sravan Kumar T: Conceptualization (equal); Data curation (equal); Formal analysis (equal); Investigation(equal); Methodology (equal); Project administration (equal); Supervision (equal); Validation(equal); Visualization(equal); Writing–original draft (equal); Writing–review & editing (equal).

Funding: This research did not receive any specific grant from funding agencies in the public, commercial or not-for-profit sectors.

Data availability: The datasets generated during and/or analyzed during the current study are not publicly available because they comprise large simulation datasets and MATLAB source files that are not deposited in a public repository. However, they are available from the corresponding author on reasonable request.

Declarations:

Ethics approval and consent to participate Not applicable. This study does not involve any human participants, animals, or identifiable personal data.

Consent for publication

Consent to publish: not applicable.

Generative AI and AI-assisted technologies in the writing process:

During the preparation of this work, the authors used OpenAI tools and Grammarly in order to enhance grammar, and readability. After using these tools, the authors reviewed and edited the content as needed and take full responsibility for the content of the publication.

Competing interest: The authors declare no competing interests.

Clinical Trial Registration: Not applicable. No clinical trial was conducted, and no human participants were involved in this study.

Nomenclature

B_0	Magnetic field strength, T		**Greek symbols**
C_p	Specific heat $\left(kJ/kg.K\right)$	ω	Constant rotation velocity, (rad/s)
Da	Darcy number	α	Thermal diffusivity $\left(m^2/s\right)$
Ec	Eckert number	ϕ	Solid volume fraction
F	Forcheimer drag	μ	Dynamic viscosity $\left(Pa.s\right)$
Ha	Hartmann number	ρ	Density $\left(kg/m^3\right)$
N	Radiation parameter	η	Aspect ratio
Nu	Nusselt number	θ	Dimensionless temperature (K)
Pr	Prandtl number	υ	Kinematic Viscosity, (m^2/s)
Q	Internal heat sink parameter	κ	Thermal conductivity of fluid. (W/m. K)
q_r	Radiative heat flux	β	Thermal expansion coefficients. (K^{-1})
R	Radial axis	σ	Electrical conductivity, (S/m)
Re	Reynolds number		**Subscripts**
r_1	Radius of the inner cylinder, (m)	nf	Nanofluid
r_2	Radius of the outer cylinder, (m)	f	Base fluid

T	Dimensional temperature (K)	s	Solid nanoparticles
U	Dimensional velocity, (ms^{-2})		
u	Non - dimensional velocity, (ms^{-2})		

References

[1] Choi, S. U. S., Eastman, J. A. Enhancing thermal conductivity of fluids with nanoparticles. *ASME International Mechanical Engineering Congress and Exposition.* 1995.

[2] Ali, A., Das, S., Jana, R.N. (2023). MHD gyrating stream of non-Newtonian modified hybrid nanofluid past a vertical plate with ramped motion, Newtonian heating and Hall currents. *ZAMM - Journal of Applied Mathematics and Mechanics*, 2023, *103*(9):1-15. https://doi.org/10.1002/zamm.202200080

[3] Sunder, M. R., Shamshuddin, M.D., Satyanarayana, C., Salawu, S.O. Stagnation point flow for the dynamics of thermal enhancement in nanofluid by a convective extending surface with suction/injection and heat source. *International Journal of Modern Physics B*, 2024, *38*(31):1-15. https://doi.org/10.1142/s021797922450423x

[4] Mahros, A.M., Aly, E.H. Comparative study for heat transfer characteristics of many graphene hybrid nanofluids flow over a shrinking sheet. *Chinese Journal of Physics*, 2024, *92*: 416–431. https://doi.org/10.1016/j.cjph.2024.08.010

[5] Roopa, K. R., Dinesh, P. A., Yadav, S., Makinde, O. D. Influence of radiative heat transfer on hybrid nanofluid across a curved surface with porous medium. *International Journal of Numerical Methods for Heat & Fluid Flow*, 2025, *35*(3): 1093–1115. https://doi.org/10.1108/hff-05-2024-0360

[6] Nayak, K., Rani, H. P., Rameshwar, Y., Devanuri, J. K. Weakly nonlinear analysis of rotating magnetoconvection with anisotropic thermal diffusivity effect. *Physics of Fluids*, 2024, *36*(7):1-15. https://doi.org/10.1063/5.0217532

[7] Sampath Kumar, P., Hanumagowda, N., Pavithra, K. M., Varma, S. V. K., Hemanth, K. Thermal and flow analysis of bi-viscosity hybrid nanofluid between rotating disks under viscous dissipation and quadratic radiation effects: RSM approach. *International Journal of Ambient Energy*, 2025, *46*(1): 1-12. https://doi.org/10.1080/01430750.2025.2503285

[8] Madangningdang, T., Hanumagowda, B. N., Prasad, K. V., Subray P. V. A. Sensitivity analysis of convective–radiative permeable annular fin with variable emissivity and internal heat generation using RSM-CCD. *Pramana*, 2025, *99*(3): 1-12. https://doi.org/10.1007/s12043-025-02944-1

[9] Saranya, S., Al-Mdallal, Q. M. Non-Newtonian ferrofluid flow over an unsteady contracting cylinder under the influence of aligned magnetic field. *Case Studies in Thermal Engineering*, 2020, *21*: 100679. https://doi.org/10.1016/j.csite.2020.100679

[10] Hasan, N., Saha, S., Umavathi, J. C. Magnetohydrodynamic convection in a heat-generating ferrofluid within a corrugated cavity containing a rotating cylinder. *Physics of Fluids*, 2024, *36*(7): 1-12. https://doi.org/10.1063/5.0216132

[11] Umavathi, J. C., Sheremet, M. A., Subray, A. Response surface optimization of heat transfer in magnetic nanofluid flow within a permeable square enclosure: Corrugated wall and Joule heating effects. *Heat Transfer*, 2024, *54*(1): 585–608. https://doi.org/10.1002/htj.23189

[12] Saranya, S., Al-Mdallal, Q. M., Javed, S. Shifted Legendre Collocation Method for the Solution of Unsteady Viscous-Ohmic Dissipative Hybrid Ferrofluid Flow over a Cylinder. *Nanomaterials*, 2021, *11*(6):1512. https://doi.org/10.3390/nano11061512
[13] Umavathi, J. C., Shamshuddin, MD. Computational micropolar model of hybrid nanofluid flow across a wedge. *Numerical Heat Transfer, Part A: Applications*, 2024, *96*(1): 1–17. https://doi.org/10.1080/10407782.2024.2368273
[14] Alhefthi, R. K., Umavathi, J. C., Inc, M., Oke, A. S. Effects of radiative heat flux on MHD squeezing Newtonian flow between convectively heated parallel disks. *Pramana*, 2023, *97*(4):1-12. https://doi.org/10.1007/s12043-023-02650-w
[15] Mahesha, R., Nalinakshi, N., Kumar, T. S. Numerical study of radiative MHD hybrid nanofluid flow through porous concentric cylinders. *Archives of Thermodynamics*, 2025, *4*(1): 201–201. https://doi.org/10.24425/ather.2025.154194
[16] Rajeev, A., Puneeth, V., Manjunatha, S., Makinde, O.D. Magnetohydrodynamic flow of two immiscible hybrid nanofluids between two rotating disks. *Numerical Heat Transfer, Part A: Applications*, 2024, 86(13): 4305–4323.
https://doi.org/10.1080/10407782.2024.2317436
[17] Sankari, M. S., Rao, M. E., Khan, W., Makinde, O. D., Awwad, F. A., Ismail, E. A. A. Activation energy and motile microorganism influence on MHD Jeffery nanofluid with stratifications. *AIP Advances*, 2025, *15*(5):1-12. https://doi.org/10.1063/5.0221168
[18] Ashrith, R. P., Nagaraja, K. V., Neelima, N., Prasad, K. V., Kulshreshta, A., Makinde, O. D. Thermal analysis of MHD non-Newtonian nanofluid flow across a Riga parallel plate with Cattaneo-Christov heat flux: A deep learning approach. *International Journal of Thermofluids*, 2025, *27*: 101194. https://doi.org/10.1016/j.ijft.2025.101194
[19] Ben Khedher, N., Ullah, Z., Alam, M. M., Al-Arni, S., Elbadawi, I., Makinde, O. D. Significance of thermal conductivity and variable density on heat and mass transfer of MHD second-grade nanofluid along high-temperature polymer surface. *Case Studies in Thermal Engineering*, 2025, *71*: 106168. https://doi.org/10.1016/j.csite.2025.106168
[20] Khan, I., Chinyoka, T., Zulkifli, R., Ismail, E. A. A., Awwad, F. A., Hassan, A. M. Correction: Numerical study of unsteady reactive third-grade fluid flow in a microchannel through a porous medium subject to exothermic reaction. *Pramana*, 2025, *99*(2): 1-12.
https://doi.org/10.1007/s12043-025-02905-8
[21] Gosty, V., Srinivas, G., Babu, B. S. Numerical Investigation of Slip Effects on Heat and Mass Transfer in a Vertical Channel with Immiscible Micropolar and Viscous Fluids of Variable Viscosity. *Partial Differential Equations in Applied* Mathematics, 2024, *13*: 101139. https://doi.org/10.22541/au.171862351.17757003/v1
[22] Kumar, T. S. Analytical and numerical solution of MHD flow and heat transfer of a viscoelastic fluid in wire coating analysis. *Discover Applied Sciences*, 2024, *7*(2): 142.
https://doi.org/10.21203/rs.3.rs-5288567/v1
[23] Sohail, M., Naz, R. Modified heat and mass transmission models in the magnetohydrodynamic flow of Sutterby nanofluid in stretching cylinder. *Physica A: Statistical Mechanics and its Applications*, 2020, *549:* 124088.
https://doi.org/10.1016/j.physa.2019.124088

[24] Ghasemi, S. E., Hatami, M. Solar radiation effects on MHD stagnation point flow and heat transfer of a nanofluid over a stretching sheet. *Case Studies in Thermal Engineering*, 2021, *25:* 100898. https://doi.org/10.1016/j.csite.2021.100898
[25] Gouran, S., Mohsenian, S., Ghasemi, S. E. Theoretical analysis on MHD nanofluid flow between two concentric cylinders using efficient computational techniques. *Alexandria Engineering Journal*, 2022, *61*(4): 3237–3248. https://doi.org/10.1016/j.aej.2021.08.047
[26] Peng, Y., Alsagri, A. S., Afrand, M., Moradi, R. A numerical simulation for magnetohydrodynamic nanofluid flow and heat transfer in rotating horizontal annulus with thermal radiation. *RSC Advances*, 2019, *9*(39): 22185–22197.
https://doi.org/10.1039/c9ra03286j
[27] Sravan Kumar, T., Dinesh, P. A., Makinde, O. D. Impact of Lorentz force and viscous dissipation on unsteady nanofluid convection flow over an exponentially moving vertical plate. *Mathematical Models and Computer Simulations*, 2020, *12*(4): 631–646.
https://doi.org/10.1134/s2070048220040110
[28] Babu, P. R., Kumar, M. A., Raju, R. S., Reddy, Y. D. Numerical solutions of steady radiative Maxwell-nanofluid flow toward a stretching sheet in the presence of magnetic field and porous medium. *Modern Physics Letters B*, 2024, *39*(8): 1-15.
https://doi.org/10.1142/s0217984924504323
[29] Mahesha. R., Thavada, S. K., Aly, E. H. Thermal radiation effect on magneto-hydrodynamic nanofluid flow over a rotating horizontal annulus with porous medium. *Nano*, 2025, *44*(1): 1-12. https://doi.org/10.1142/s1793292025500547
[30] Bruggeman, D. A. G. Berechnung verschiedener physikalischer kon stanten von heterogenen substanzen, I. Dielektrizitatskonstanten und leitfahig keiten der mischkorper aus isotropen substanzen. *Annalen der Physik*, 1935, *416:* 636-664.
https://doi.org/10.1002/andp.19354160705

Supplementary Files

This is a list of supplementary files associated with this preprint. Click to download.

- GraphicalResultsandDiscussion.docx